Progress In Electromagnetics Research Letters, Vol. 102, 109–117, 2022

Low Losses and Compact Size Microstrip Diplexer Based on Open-Loop Resonators with New Zigzag Junction for 5G Sub-6-GHz and Wi-Fi Communications

Souhaila Ben Haddi[1, *], Asmaa Zugari[2], and Alia Zakriti[1]

Abstract—In this paper, a high-performance microstrip diplexer is designed and manufactured. The design is based on two pairs rectangular open-loop resonators band-pass filters and a novel zigzag junction. It operates at 3.5 GHz for the fifth-generation (5G) sub-6-GHz and 5 GHz for Wi-Fi communications. The proposed diplexer is considerably miniaturized with a global compact size of $30 \times 17\,\text{mm}^2$. In addition, it presents low insertion losses less than 0.5 dB at both channels in comparison with the previous diplexers. Moreover, the isolation is higher than 20 dB, and the return loss is better than 14 dB at the bandwidths. To confirm the simulation results, the presented diplexer is manufactured and measured where a good agreement is observed.

1. INTRODUCTION

In the last few years, the development of the mobile communication systems has led to the apparition of the new fifth-generation (5G) after standard 4G [1–3]. Opposing the other generations, 5G is addressed in different domains, among them medicine, media, and industries [4]. On the other hand, the main role of the 5G is to change the world by linking everything together such as machines, objects, and devices. For this reason, 5G achieves high speed, great reliability, and raised availability. Furthermore, 5G wireless technology provides perfect and high performances and improved efficiency, which allow connecting the new industry 4.0 [5]. In addition, the frequency bands in 5G are split into two classes; the first one is below 6 GHz and the second one above 20 GHz and up to 80 GHz at sundry bands. The low frequency band 6 GHz can be used promptly due to the use of the current structures of wireless communication.

Recently, microstrip devices such as antennas [6], filters [7–9], power dividers [10], and diplexers [10–12] are broadly demanded for communications systems with small size and excellent performances. In this context, diplexers are considered as essential components in microwave communication systems such as satellite communication systems, radar systems, and cellular phones [13].

Diplexers are based on two bandpass filters with different frequencies and a common junction. They are used to separate the input signal into two output signals or combine two output signals into the input signal. Several models of filters are recommended for the diplexer's design, such as coupled line, quarter and half waveguide resonators, stepped impedance resonators, and interdigital cells [8, 14–17]. Moreover, these filters should be combined using common techniques which are T-junction and Y-junction [18] to realize the diplexer topology.

The microstrip diplexers mentioned in [19–24] have large sizes, which is considered a common disadvantage. In [19], a microstrip diplexer based on coupled stepped impedance resonators is presented.

Received 3 December 2021, Accepted 17 January 2022, Scheduled 28 January 2022

* Corresponding author: Souhaila Ben Haddi (souhabenhaddi2@gmail.com).

[1] Laboratory of Sciences and Advanced Technology, Department of Civil and Industrial Sciences and Technologies, National School of Applied Sciences, University of Abdelmalek Essaâdi, Tetuan, Morocco. [2] Laboratory of Information System and Telecommunication, Abdelmalek Essaâdi University, Tetuan, Morocco.

It is operated for the digital communication system and Industrial Scientific and Medical bands at 1.8 GHz and 2.45 GHz, respectively. It has a large size about $47 \times 24\,\text{mm}^2$ and high insertion losses about 2 dB at both lower and upper bands. In [20], a coupled line stepped impedance resonator is used to achieve a diplexer. It is designed for WiMAX and wireless technological advances with an overall size of $75 \times 14\,\text{mm}^2$, and the insertion losses are about 0.8 and 0.9 dB. The presented diplexers in [21] and [22] are based on open-loop resonators. They exhibit good isolation between channels, though high insertion losses and large size are introduced. A novel diplexer based on two coupled meandrous open-loop resonators is studied in [23]. It operates at 1.67 GHz for FDD schemes and 1.88 GHz for GSM applications. It presents good return loss and low insertion losses at both channels, but the isolation should be improved. In [24], a microstrip diplexer based on open-loop resonator is introduced. It operates at 1.8 and 1.9 GHz for mobile communication. The diplexer presents a large size and high insertion losses about 2.88 and 2.95 dB.

In this work, we design a compact microstrip diplexer based on two pairs of rectangular open-loop resonators band-pass filters. A novel zigzag junction combines these filters in order to obtain a compact microstrip diplexer, which occupies only $30 \times 17\,\text{mm}^2$. The main goal of the introduced diplexer is to solve the problems of the previously published diplexers especially in terms of size and insertion losses. The design procedure is organized as follows. Firstly, we design two rectangular open-loop resonators band-pass filters. Secondly, we integrate these filters by a new zigzag junction in order to obtain a miniaturized diplexer for 5G sub-6-GHz and Wi-Fi communication. Finally, we manufacture and measure the presented diplexer to validate the simulation results.

2. FILTER DESIGN

As mentioned above, the diplexer procedure starts with the design of the two bandpass filters. In fact, compact filters are generally required for wireless communication systems. Microstrip open-loop resonators with square, triangular or rectangular structures have been used broadly in the design of filters and multiplexers due to their compact and small size. For this reason, a rectangular open-loop resonator bandpass filter is proposed in this work as depicted in Figure 1(a). According to the previous work, the resonator's topology is obtained by folding a straight-transmission line modeled by a total electrical length θ_T and a characteristic impedance Z. As the topology is symmetric, the analysis of the even and odd modes is required [25].

The equivalent transmission line model of the suggested rectangular open-loop resonator is depicted in Figure 1(b). As shown, the proposed open-loop resonator is modeled by two transmission lines with

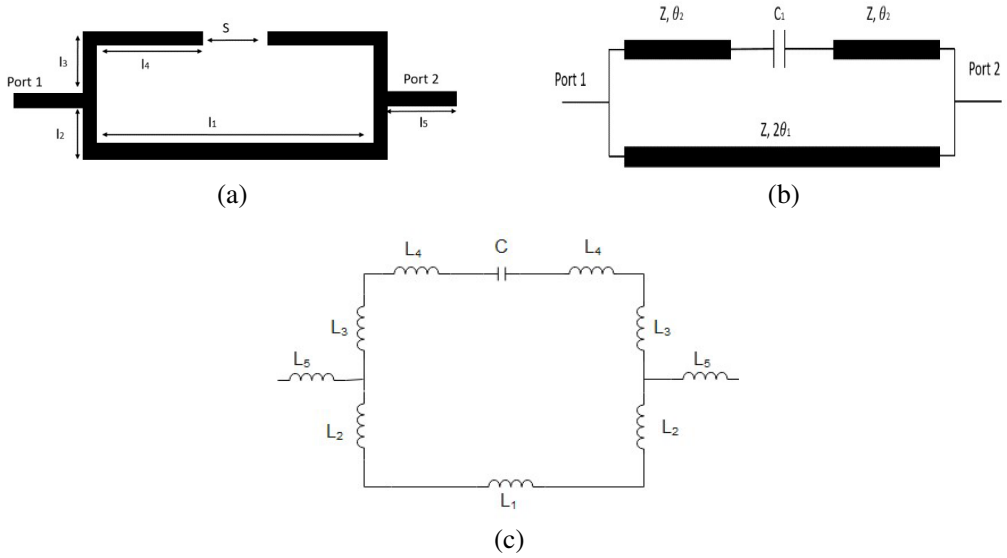

Figure 1. (a) Structure of the rectangular open-loop resonator. (b) The equivalent transmission lines model. (c) The LC model of the rectangular open-loop resonator.

two different electrical lengths θ_1, θ_2 and the same characteristics impedance Z whereas the width of the introduced resonator is constant. Moreover, the capacitance C_1 models the coupling between the two transmission lines of the resonator.

The conversion of the proposed microstrip open-loop resonator to the LC model is not difficult by using the circuit LC analysis. The equivalent LC model is displayed in Figure 1(c). As seen in this figure, the parameters L_1, L_2, L_3, L_4, and L_5 present the inductances modeling the transmission lines l_1, l_2, l_3, l_4, and l_5. Moreover, the gap S between the two lines is modeled by capacitance C. The equations for calculating the inductance and the capacitance values are given in [25].

Based on the structure given above, a pair of rectangular open-loop resonators is proposed in this work as shown in Figure 2(a). Its LC model can be performed based on the same concept given above as depicted in Figure 2(b), where M_{12} indicates the coupling coefficient between the two resonators. The dimensions (length l and width w) of the resonators in microstrip technology depend on the characteristics of the substrate and metallization, and they are calculated using the following equations [16]:

$$w = \frac{2}{\pi}h\left[(B-1) - \ln(2B-1) + \frac{\varepsilon_r - 1}{2\varepsilon_r}\left[\ln(B-1) + 0.39 - \frac{0.61}{\varepsilon_r}\right]\right] \tag{1}$$

$$l = \frac{\lambda}{2} = \frac{\lambda_0}{2\sqrt{\varepsilon_r}} \tag{2}$$

where,

$$B = \frac{60\pi^2}{Z_c\sqrt{\varepsilon_r}}, \quad \lambda_0 = \frac{C}{f_0} \tag{3}$$

given that h is the thickness of the substrate, and ε_r is the permittivity of the substrate.

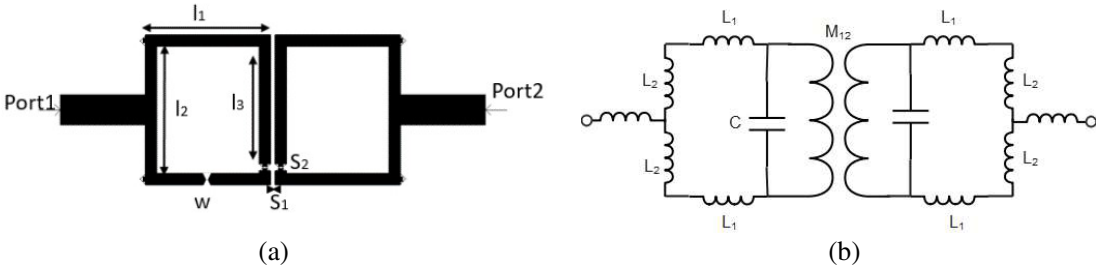

Figure 2. (a) Structure of the open-loop resonator. (b) Equivalent circuit of the open-loop resonator.

The design and optimization of the rectangular open-loop resonators bandpass filters are achieved using ADS Agilent. The first filter operates at 3.5 GHz; it has a wide upper rejection band to avoid interference with the frequency of the other filter, which operates at 5 GHz. For the same reason, the second filter should have a wide lower rejection band to obviate the intrusion with the first one.

The filters are excited by a 50 Ω microstrip line. The dielectric substrate employed is FR-4 with a dielectric constant of 4.3 and a thickness of 0.8 mm. Table 1 displays the optimized parameters; length (l_i), width (w_i), and spacing (S_{ij}) of the open-loop resonators.

Figure 3 presents the simulation of the two BPFs, and the bandwidth of the first bandpass filter is from 3.2 to 3.9 GHz. The bandwidth of the second bandpass filter is from 4.6 to 5.8 GHz. The fractional bandwidths of the band pass filters are 17% and 23%, respectively. In addition, the filters exhibit very good features, low insertion losses about 0.3 dB and good return losses which are about 25 dB and 32 dB, respectively. These performances prove that these filters are suitable for the design of a microstrip diplexer.

3. DIPLEXER DESIGN

This section focuses on the diplexer design. Its topology is established by integrating the simulated open-loop resonators bandpass filters by zigzag junction as illustrated in Figure 4. Moreover, we place

Table 1. Dimensions of both BPF1 and BPF2.

	BPF1	BPF2
l_1 (mm)	5.91	4.03
l_2 (mm)	7.03	4.94
l_3 (mm)	6.055	4.29
w (mm)	0.555	0.39
S_1 (mm)	0.2	0.2
S_2 (mm)	0.32	0.21

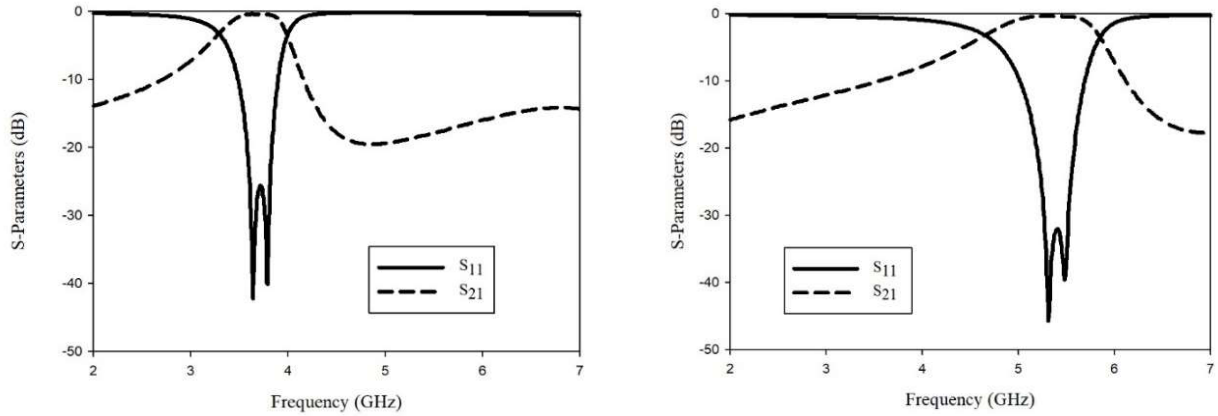

Figure 3. Simulation response of (a) BPF1 and (b) BPF2.

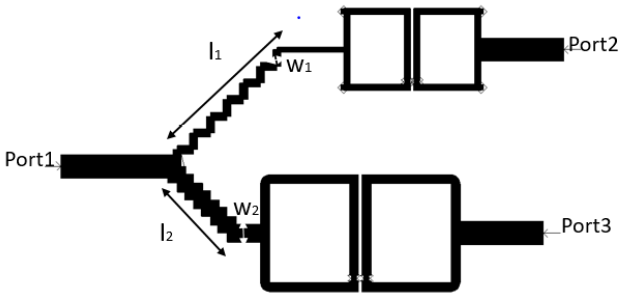

Figure 4. Structure of the proposed diplexer.

accurately the two pairs open-loop resonators bandpass filters with different sizes by the proposed zigzag junction, in a manner that each bandpass filter is linked to a branch of the junction. The final size of the diplexer is approximately $30 \times 17\,\text{mm}^2$.

The proposed diplexer has been simulated and fabricated on an FR4 substrate with the relative permittivity of 4.3, thickness of 0.8 mm, and loss tangent of 0.025. The proposed diplexer was simulated using ADS Agilent. The required frequencies are $f_1 = 5\,\text{GHz}$ and $f_2 = 3.5\,\text{GHz}$ for ports 2 and 3, respectively. These frequencies have been chosen due to the fifth-generation applications and Wi-Fi communications frequency bands which are exhibited in the literature.

The optimized parameters (lengths l_1, l_2 and widths w_2, w_3) of the proposed zigzag junction are approximated to a quarter of the guided wavelength of the two BPFs frequency bands as recapitulated in Table 2.

Table 2. Dimensions of zigzag junction.

l_1 (mm)	12
l_2 (mm)	8
$w_1 = w_2$ (mm)	0.3

A parametric study is proposed in order to investigate the effect of the zigzag junction widths (w_1 and w_2) on the diplexer performances by keeping the lengths (l_1 and l_2) constant. As shown in Figures 5, 6, and 7, the values of w_1 and w_2 given in Table 2 present insufficient performances. It can be observed from Figure 5 that the reflection coefficient S_{11} is about -7 dB and -9 dB, respectively in two passbands [3.2–3.9] GHz and [4.6–5.8] GHz. According to Figures 6 and 7, the transmission coefficients S_{21} and S_{31} are approximately -1.5 dB and -0.9 dB.

It appears clearly from the same Figures 5, 6, and 7 that the diminution of the widths w_1 and w_2 to 0.1 mm decreases the diplexer performances; the reflection coefficient S_{11} assumes the values of -4 dB and -5 dB respectively at both the passbands, while the transmission coefficients S_{21} and S_{31} decrease to -2.5 dB and -1.9 dB, respectively. Then, the increase of w_2 to 1.1 mm by keeping w_1 constant ($w_1 = 0.3$ mm) ameliorates the lower band performances of both reflection S_{11} and transmission S_{21} coefficients to -11 dB and -0.8 dB, respectively. Similarly, the augmentation of w_1 to 0.5 mm (with $w_2 = 0.3$ mm) improves the upper band performances. As seen, the reflection coefficient S_{11} is about -13 dB, whereas the transmission coefficient S_{31} is approximately -0.4 dB. Once the widths w_1 and w_2 increase to 0.5 mm and 1.1 mm, respectively, the reflection coefficient S_{11} is enhanced to -24 dB and -16 dB respectively at the lower and upper bands. Furthermore, the transmission coefficients S_{21} and S_{31} are about 0.3 dB at both bands, which proves that the diplexer performances are perfect when $w_2 = 1.1$ mm and $w_1 = 0.5$ mm.

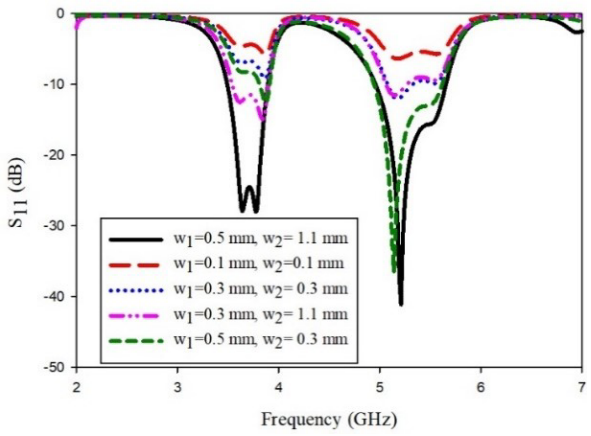

Figure 5. Simulated S_{11} with varied widths.

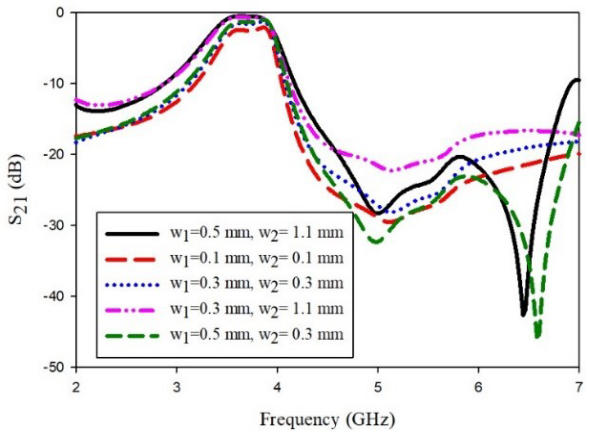

Figure 6. Simulated S_{21} with varied widths.

4. RESULTS AND DISCUSSION

The fabricated diplexer prototype is shown in Figure 8. It was manufactured using the circuit-board plotter LPKF ProtoMat E33. The S-parameters were measured by a Rohde and Schwarz ZVB 20 vector network analyzer. Note that the frequency range of this analyzer is confined to 20 GHz. In addition, it has just two ports; therefore, the third port of the diplexer is connected to 50 Ω load when we measure the other two ports as indicated in Figure 9.

The simulated and measured reflection coefficients S_{11} are displayed in Figure 10. The transmission coefficients S_{21} and S_{31} are depicted in Figure 11, whereas the measured and simulated isolations S_{23} are displayed in Figure 12. High correlation between simulated and measured data is observed with

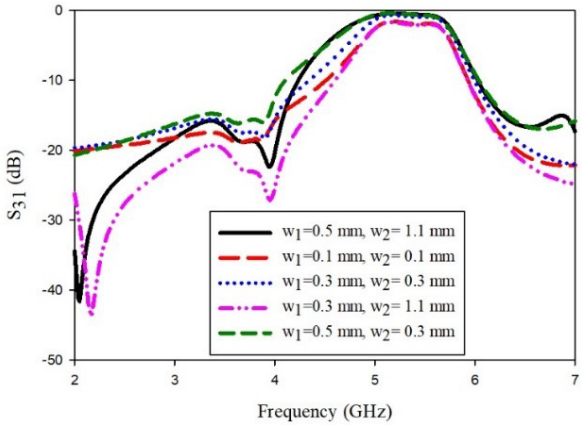

Figure 7. Simulated S_{31} with varied widths.

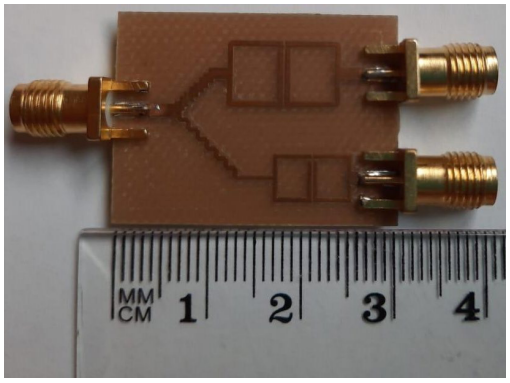

Figure 8. Microstrip diplexer prototype.

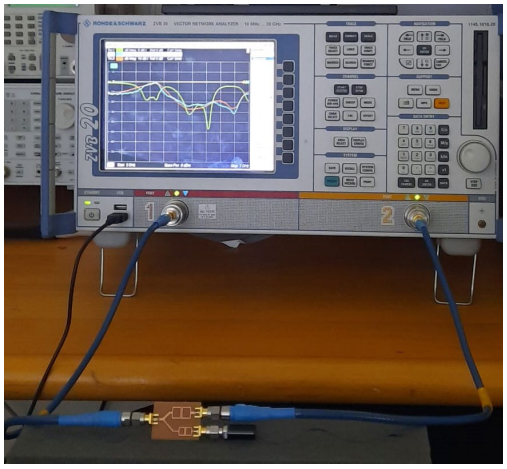

Figure 9. Measurement of the designed diplexer.

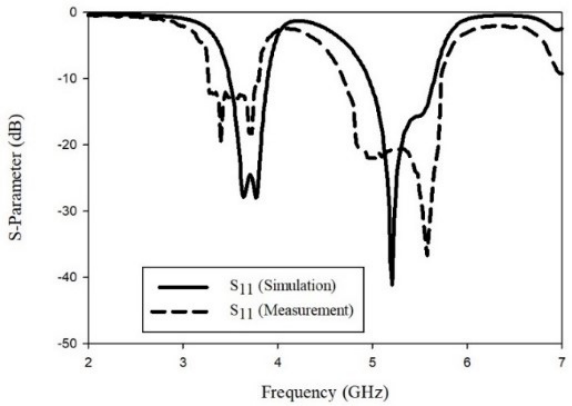

Figure 10. Simulated and measured S_{11}.

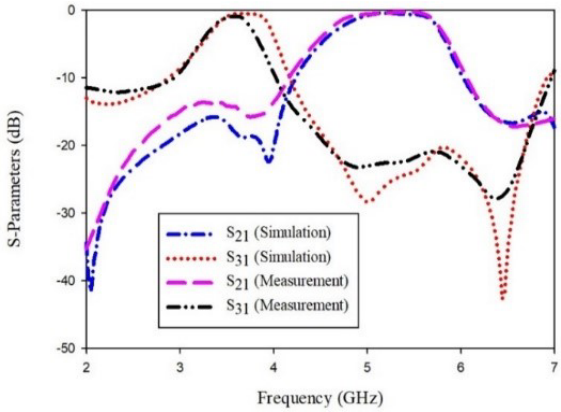

Figure 11. Simulated and measured S_{21} and S_{31}.

petty frequency shift due to possible manufacturing errors and physical environment conditions at the time of measurement.

As seen from Figures 10, 11, and 12, when signal is applied to input port (port 1), then it comes out of the two output ports (port 2 and port 3) in two different central frequencies with a low insertion

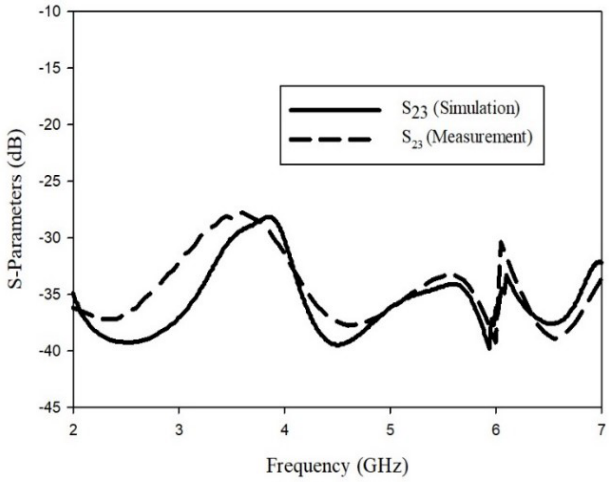

Figure 12. Simulated and measured S_{23}.

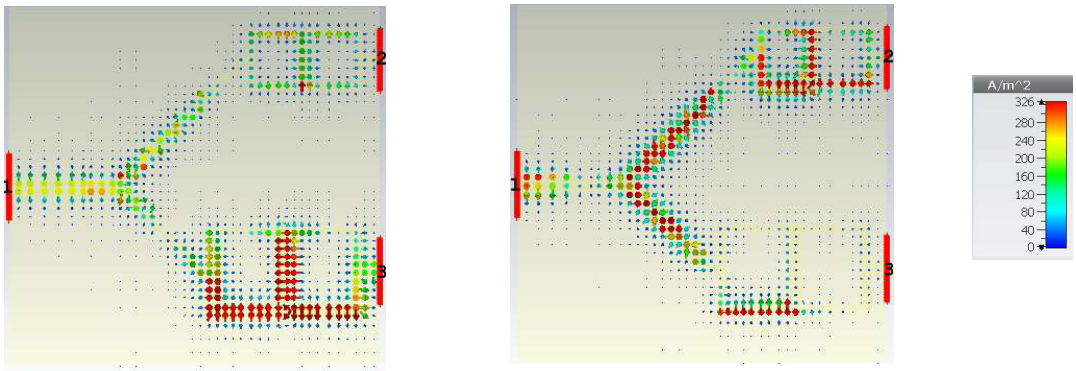

(a) (b)

Figure 13. Current distribution of the proposed diplexer (a) at 3.5 GHz, (b) at 5 GHz.

losses S_{21} and S_{31} of 0.43 dB and 0.48 dB, respectively. The return loss of the input port (port 1) at the operated frequencies is about 14 dB and 20 dB which is appropriate for diplexing. As depicted in Figure 12, the isolation between the two channels is about 20 dB which is great and suitable for the designed diplexer. The fractional bandwidths at lower and higher frequencies were around 17% and 23%, respectively. The presented diplexer is electrically small compared to traditional diplexers based on open-loop resonators.

Figure 13 displays the current distribution for the introduced diplexer at two operational frequencies. As observed from Figure 13(a), the concentration of the current at the lower band is very high compared to the upper band when the proposed diplexer operates at 3.5 GHz. In the same way, the concentration of the current at the upper band is more important than the lower band when the designed diplexer operates at 5 GHz as seen in Figure 13(b).

Table 3 summarizes a comparison between our proposed diplexer and other diplexers based on open-loop resonators proposed in literature. As can be observed, our introduced diplexer presents low insertion losses at both channels in comparison with [21] and [22] and high isolation compared with [23]. In addition, the proposed diplexer is characterized by a compact size of $30 \times 17\,\text{mm}^2$ compared with [21] and [22]. Otherwise, compared to [21] and [22] the isolation between the two channels of our diplexer should be enhanced.

Table 3. Comparison performances.

Refs/Year	Lower/Higher channels (GHz)	Insertion losses (dB)	Isolation (dB)	Size (mm^2)	FBW (%)
[23]/2020	1.67/1.88	0.43/0.35	22.13	27.5×22.3	1.79/2.12
[22]/2014	2.45/5.14	2/3.7	35	52×20	8.1/4.46
[21]/2016	2.34/2.59	1.5/1.3	31	34×24	3.6/3.4
[This work]	3.5/5	0.43/0.48	28	30×17	17/23

5. CONCLUSION

In this paper, a compact microstrip diplexer has been designed, manufactured, and measured. It is based on two pairs of rectangular open-loop resonators. The realization of this structure has been achieved by combining the two filters by a zigzag junction. The desired frequencies are 3.5 GHz and 5 GHz for ports 3 and 2, respectively. According to the results, the presented diplexer has the advantages of compact size of $30 \times 17\,mm^2$ and low insertion losses of 0.4 dB compared to the other works. This presented structure is very attractive for fifth-generation applications and Wi-Fi communications.

REFERENCES

1. Ezhilarasan, E. and M. Dinakaran, "A review on mobile technologies: 3G, 4G and 5G," *2017 Second International Conference on Recent Trends and Challenges in Computational Models (ICRTCCM)*, 369–373, 2017.
2. Yu, H., H. Lee, and H. Jeon, "What is 5G? Emerging 5G mobile services and network requirements," *Sustainability*, Vol. 9, No. 10, 1848, 2017.
3. Kim, D., "A 2020 perspective on 'A dynamic model for the evolution of the next generation Internet-Implications for network policies': Towards a balanced perspective on the Internet's role in the 5G and Industry 4.0 era," *Electron. Commer. Res. Appl.*, Vol. 41, 100966, 2020.
4. Magsi, H., A. H. Sodhro, F. A. Chachar, S. A. K. Abro, G. H. Sodhro, and S. Pirbhulal, "Evolution of 5G in Internet of medical things," *2018 International Conference on Computing, Mathematics and Engineering Technologies (iCoMET)*, 1–7, 2018.
5. Rao, S. K. and R. Prasad, "Impact of 5G technologies on industry 4.0," *Wirel. Pers. Commun.*, Vol. 100, No. 1, 145–159, 2018, doi: 10.1007/s11277-018-5615-7.
6. Fady, B., J. Terhzaz, A. Tribak, F. Riouch, and Á Mediavilla Sánchez, "Novel miniaturized planar low-cost multiband antenna for industry 4.0 communications," *Progress In Electromagnetics Research C*, Vol. 93, 29–38, 2019.
7. Ben Haddi, S., A. Zugari, A. Zakriti, and S. Achraou, "Design of a band-stop planar filter for telecommunications applications," *Procedia Manuf.*, Vol. 46, 788–792, 2020.
8. Ben Haddi, S., A. Zugari, A. Zakriti, and S. Achraou, "A compact microstrip t-shaped resonator band pass filter for 5G applications," *2020 International Conference on Intelligent Systems and Computer Vision (ISCV)*, 1–5, 2020.
9. Achraou, S., H. Elftouh, A. Farkhsi, A. Zakriti, and S. Ben Haddi, "Substrate integrated waveguide bandpass filter for mm-Wave applications," *Procedia Manuf.*, Vol. 46, 766–770, 2020.
10. Jamshidi, M., A. Lalbakhsh, S. Lotfi, H. Siahkamari, B. Mohamadzade, and J. Jalilian, "A neuro-based approach to designing a Wilkinson power divider," *Int. J. RF Microw. Comput. Eng.*, Vol. 30, No. 3, e22091, 2020.
11. Rezaei, A., L. Noori, and M. H. Jamaluddin, "Novel microstrip lowpass-bandpass diplexer with low loss and compact size for wireless applications," *AEU — International J. Electron. Commun.*, Vol. 101, 152–159, 2019.

12. Upadhyaya, T., J. Pabari, V. Sheel, A. Desai, R. Patel, and S. Jitarwal, "Compact and high isolation microstrip diplexer for future radio science planetary applications," *AEU — International J. Electron. Commun.*, Vol. 127, 153497, 2020.
13. Ghosh, P., "Microwave and satellite communications," *TEMS J. Technology Eng. Maths Sci.*, Vol. 3, No. 2, 90–91, 2021.
14. Saleh, S., W. Ismail, and I. S. Z. Abidin, "5G Hairpin and interdigital bandpass filters," *Int. J. Integr. Eng.*, Vol. 12, No. 6, 71–79, 2020.
15. Al-Yasir, Y., R. A. Abd-Alhameed, J. M. Noras, A. M. Abdulkhaleq, and N. O. Parchin, "Design of very compact combline band-pass filter for 5G applications," *The Loughborough Antennas & Propagation Conference (LAPC 2018)*, 1–4, 2018.
16. Hong, J.-S. G. and M. J. Lancaster, *Microstrip Filters for RF/Microwave Applications*, Vol. 167, John Wiley & Sons, 2004.
17. Ben Haddi, S., A. Zugari, A. Zakriti, and S. Achraou, "5G narrow-band band-pass filter using parallel coupled lines and L-shaped resonator," *2020 International Symposium on Advanced Electrical and Communication Technologies (ISAECT)*, 1–4, 2020.
18. Saieed, A., W. Pao, and H. M. Ali, "Prediction of phase separation in a T-Junction," *Exp. Therm. Fluid Sci.*, Vol. 97, 160–179, 2018.
19. Chinig, A., et al., "A new microstrip diplexer using coupled stepped impedance resonators," *Int. J. Electr. Comput. Energ. Electron. Commun. Eng.*, Vol. 9, No. 1, 41–44, 2015.
20. Yousif, A. B. and S. E. Ahmed, "A dual-band coupled line based microstrip diplexer for wireless applications," *J. Glob. Sci. Res.*, Vol. 10, 845–853, 2020.
21. Salehi, M. R., S. Keyvan, E. Abiri, and L. Noori, "Compact microstrip diplexer using new design of triangular open loop resonator for 4G wireless communication systems," *AEU — International J. Electron. Commun.*, Vol. 70, No. 7, 961–969, 2016.
22. Chinig, A., et al., "A new microstrip diplexer using open-loop resonators," *J. Microwaves, Optoelectron. Electromagn. Appl.*, Vol. 13, No. 2, 185–196, 2014.
23. Rezaei, A., S. I. Yahya, L. Nouri, and M. H. Jamaluddin, "Design of a low-loss microstrip diplexer with a compact size based on coupled meandrous open-loop resonators," *Analog Integr. Circuits Signal Process.*, Vol. 102, No. 3, 579–584, 2020.
24. Nwajana, A. O. and K. S. K. Yeo, "Microwave diplexer purely based on direct synchronous and asynchronous coupling," *Radioengineering*, Vol. 25, No. 2, 247–252, 2016.
25. Chinig, A., A. Errkik, L. El Abdellaoui, A. Tajmouati, J. Zbitou, and M. Latrach, "Design of a microstrip diplexer and triplexer using open loop resonators," *J. Microwaves, Optoelectron. Electromagn. Appl.*, Vol. 15, 65–80, 2016.